J Fluoresc (2015) 25:253–261
DOI 10.1007/s10895-015-1501-9

ORIGINAL PAPER

Membrane Effects of N-Terminal Fragment of Apolipoprotein A-I: A Fluorescent Probe Study

Valeriya Trusova · Galyna Gorbenko · Mykhailo Girych · Emi Adachi · Chiharu Mizuguchi · Rohit Sood · Paavo Kinnunen · Hiroyuki Saito

Received: 6 August 2014 / Accepted: 2 January 2015 / Published online: 18 January 2015
© Springer Science+Business Media New York 2015

Abstract The binding of monomeric and aggregated variants of 1–83 N-terminal fragment of apolipoprotein A-I with substitution mutations G26R, G26R/W@8, G26R/W@50 and G26R/W@72 to the model lipid membranes composed of phosphatidylcholine and its mixture with cholesterol has been investigated using fluorescent probes pyrene and Laurdan. Examination of pyrene spectral behavior did not reveal any marked influence of apoA-I mutants on the hydrocarbon region of lipid bilayer. In contrast, probing the membrane effects by Laurdan revealed decrease in the probe generalized polarization in the presence of aggregated proteins. suggesting that oligomeric and fibrillar apoA-I species induce increase in hydration degree and reduction of lipid packing density in the membrane interfacial region. These findings may shed light on molecular details of amyloid cytotoxicity.

Keywords Apolipoprotein A-I · Amyloid fibrils · Lipid bilayer perturbations · Fluorescent probes

V. Trusova · G. Gorbenko · M. Girych
Department of Nuclear and Medical Physics, V.N. Karazin Kharkiv National University, 4 Svobody Sq., Kharkov 61077, Ukraine

E. Adachi · C. Mizuguchi · H. Saito
Institute of Health Biosciences, Graduate School of Pharmaceutical Sciences, The University of Tokushima, 1-78-1 Shomachi, Tokushima 770-8505, Japan

R. Sood · P. Kinnunen
Department of Biomedical Engineering and Computational Science, School of Science and Technology, Aalto University, 00076 Espoo, Finland

V. Trusova (✉)
19-32 Geroyev Truda Str., Kharkov 61144, Ukraine
e-mail: valtrusova@yahoo.com

Introduction

Aberrant protein fibrillization is commonly associated with a number of devastating disorders, such as Alzheimer's, Parkinson's, and Huntington's diseases, type II diabetes, atrial amyloidosis, etc. [1–4]. These pathological linear aggregates are typically composed of misfolded proteins polymerized into amyloid fibrils sharing a core cross-β-sheet structure, in which polypeptide chains are oriented in such a way that β-strands run perpendicularly to the long axis of the fibril, while β-sheets coincide with its direction [5–8]. A vast majority of proteins and peptides, including both pathogenic and non-pathogenic ones, were shown to form the amyloid aggregates [3, 9]. Despite the ever growing number of reports linking the formation of protein amyloid self-assemblies and progression of severe disorders, the molecular details of fibril cytotoxicity still remain obscure. Ample evidence provides strong grounds for believing that disruption of cellular membrane by amyloid aggregates is one of the main mechanisms of fibril-induced cellular dysfunctions [3, 10, 11]. Modern concepts suggest that the mechanisms by which amyloidogenic proteins exert a destructive influence on membranes are similar to those of antimicrobial peptides and include carpeting, toroidal or barrel-stave pore formation, nonspecific membrane permeabilization, detergent- and raft-like membrane dissolution, etc. [12–14]. All these mechanisms are not mutually exclusive and an individual peptide may induce different processes of membrane damage depending on the membrane lipid composition. The alteration of membrane integrity, initiated by mature fibrils, may result in enhancement of lipid bilayer permeability [15], lipid loss [16], receptor activation [17], membrane fragmentation [18] and oxidation of membrane lipids [19].

Among a huge variety of amyloid-forming proteins, pathological aggregation of apolipoprotein A-I (apoA-I) is known to be responsible for the hereditary and systemic amyloidosis [20]. ApoA-I, a primary protein component of high-density

lipoproteins (HDL), plays a crucial role in lipid metabolism, delivering cholesterol to steroidogenic tissues and/or shuttling it from the periphery to the liver for catabolism (reverse cholesterol transport) [21, 22]. Naturally occurring mutations in apoA-I strongly affect normal functionality of the protein making it highly amyloidogenic. Specifically, in vivo formation of amyloid deposits of 16 variants of apoA-I was shown to be directly associated with the development of familial hypercholesterolemia and autosomal dominant systemic amyloidosis [23]. In most cases apoA-I fibrils are mainly composed of N-terminal fragment of the protein [24, 25]. Specifically, N-terminal 1–83 sequence has been identified to play crucial role in amyloid formation. It was found that G26R point mutation (Iowa mutation) strongly enhances the amyloid formation of N-terminal region of apoA-I [26, 27]. The molecular basis of the accelerated rate of fibril growth is supposed to lie in the disruption of apoA-I helix bundle and structural reorganization of the mutated protein resulting in the exposure of hydrophobic patches and increased propensity of the G26R mutant to form intramolecular H-bonds which stabilize the fibrillar aggregates [28]. Though the structural peculiarities of amyloid fibrils of apoA-I Iowa variant has been reported recently, the molecular-level details of its interactions with lipid membranes are still lacking.

In the present work we explored the effect of N-terminal fragments of the wild (1–83) and amyloidogenic variants of apoA-I with substitution mutations 1-83/G26R, 1-83/G26R/W@8, 1-83/G26R/W@50 and 1-83/G26R/W@72 on the structural and dynamical properties of lipid membranes. Membrane systems were represented by lipid vesicles composed of neat phosphatidylcholine (PC) and PC mixtures with 30 mol% of cholesterol (Chol). To evaluate the extent of bilayer modification, two fluorescent probes, differing in their spectral properties and membrane location, viz. pyrene and Laurdan, have been recruited.

Materials and Methods

Materials

The N-terminal 1–83 fragment of human apoA-I 1-83/G26R and its single tryptophan variants G26R/W@8, G26R/W@50 and G26R/W@72 were expressed and purified as described elsewhere [29]. The amino acid sequences of the mutants are given in Table 1. The apoA-I preparations were at least 95 % pure as assessed by SDS-PAGE.

Egg yolk phosphatidylcholine and cholesterol were purchased from Avanti Polar Lipids (Alabaster, AL). Pyrene was from Sigma (St. Louis, MO, USA), Laurdan (6-Lauroyl-2-dimethylaminonaphthalene) was from Invitrogen Molecular Probes (Eugene, OR, USA).

Table 1 Amino acid sequences of apoA-I mutants

ApoA-I mutant	Amino acid sequence
wild-type 1–83	DEPPQSPWDRVKDLATVYVDVLKDSGRDYVS QFEGSALGKQLNLKLLDNWDSVTSTFSK LREQLGPVTQEFWDNLEKETEGLR
1-83/G26R	DEPPQSPWDRVKDLATVYVDVLKDS**R**RDYV SQFEGSALGKQLNLKLLDNWDSVT STFSKL REQLGPVTQEFWDNLEKETEGLR
1-83/G26R/W@8	DEPPQSPWDRVKDLATVYVDVLKDS**R**RDYV SQFE GSALGKQLNLKLLDN**F**DSVTSTFSKL REQLGPVTQEF**F**DNLEKETEGLR
1-83/G26R/ W@50	DEPPQSP**F**DRVKDLATVYVDVLKDS**R**RDYV SQFEGSALGKQLNLKLL DNWDSVTSTF SKLREQLGPVTQEF**F**DNLEKETEGLR
1-83/G26R/ W@72	DEPPQSP**F**DRVKDLATV YVDVLKDS**R**RDYV SQFEGSALGKQLNLKLLDN**F**DSVTSTFSKL REQLGPVTQEFWDNLEKETEGLR

Given in bold font is the substituted amino acid

Preparation of Amyloid Fibrils

In all experiments, apoA-I variants were freshly dialyzed from 6 M guanidine hydrochloride solution into 10 mM Tris buffer, 150 mM NaCl, 0.01 % NaN_3, pH 7.4 before use. The reaction of protein fibrillization was conducted at 37 °C in the above buffer with constant agitation on an orbital shaker. The amyloid nature of fibrillar aggregates was confirmed in Thioflavin T (ThT) assay [30].

Preparation of Lipid Vesicles

Large unilamellar vesicles were prepared from PC and PC/Chol mixture using extrusion technique. The thin lipid film was obtained by evaporation of lipid ethanol solutions and then hydrated with 1.2 ml of 10 mM Tris buffer, 150 mM NaCl, 0.01 % NaN_3 to yield final lipid concentration 5 mM. Subsequently, lipid suspension was extruded through a 50 nm pore size polycarbonate filter.

Fluorescence Measurements

Fluorescence measurements were performed with a LS-55 spectrofluorimeter equipped with a magnetically stirred cuvette holder (Perkin-Elmer Ltd., Beaconsfield, UK) using 10 mm path-length quartz cuvettes. Emission spectra were recorded with excitation wavelengths of 340 nm for pyrene and 364 nm for Laurdan.

The ratio of vibronic bands in the pyrene fluorescence spectra (I_I/I_{III}) was calculated from the intensities at 371 nm (I) and 383 nm (III). The excimer-to-monomer fluorescence intensity ratio (E/M) was determined by measuring fluorescence intensity at the monomer (390 nm) and excimer

(460 nm) peaks. The Generalized Polarization (GP) of Laurdan fluorescence was determined as [31]:

$$GP = \frac{I_B - I_R}{I_B + I_R} \quad (1)$$

where I_B and I_R are the maximum fluorescence intensities of the blue (440 nm) and red (490 nm) spectral components, respectively.

Transmission Electron Microscopy

For electron microscopy assay, a 10 μl drop of the protein solution was applied to a carbon-coated grid and blotted after 1 min. A 10 μl drop of 2 % (*w*/*v*) uranyl acetate solution was placed on the grid, blotted after 30 s, and then washed 3 times by deionized water and air dried. The resulting grids were viewed at Jeol JSM-840 or Tecnai 12 BioTWIN electron microscope.

Results

General Characterization of apoA-I Amyloid Variants

At the first stage of the study we characterized the amyloid fibrils in the absence of lipid vesicles. In transmission electron microscopy images fibrillar self-assemblies prepared from apoA 83 mutants were visualized as rod-like structures of 5–10 nm in width and of different lengths (Fig. 1a). Previously we suggested that protofilaments of apoA-I 1–83 fibrils possess the U-shape form in which two tentative β-strands embracing the regions L14–V31 and Q41–S58 form self-complementary steric zipper, stabilized by van der Waals and hydrophobic interactions together with tentative salt bridge between R27 and D48 [32].

The amyloidogenic potentials of apoA-I variants were analyzed with Thioflavin T (ThT) assay. Association of the amyloid aggregates with this dye resulted in the expected increase of ThT emission. The kinetic profiles of ThT fluorescence in the presence of the examined apoA-I variants displayed distinct propensities for fibril formation, with fibrillization extent increasing in the order: 1–83–1-83/G26R/W@72–1-83/G26R/W@50–1-83/G26R–1-83/G26R/W@8 (Fig. 1b, c). Since the employed fibrillization conditions involved orbital shaking of the protein samples during prolonged (more than 2-week period), it seemed logical to assume that even when ThT fluorescence did not undergo sigmoidal growth, as in the cases of 1–83 and 1-83/G26R/W@72, all shaked samples contain aggregated protein species, but differ in the proportion of oligomers and fibrils.

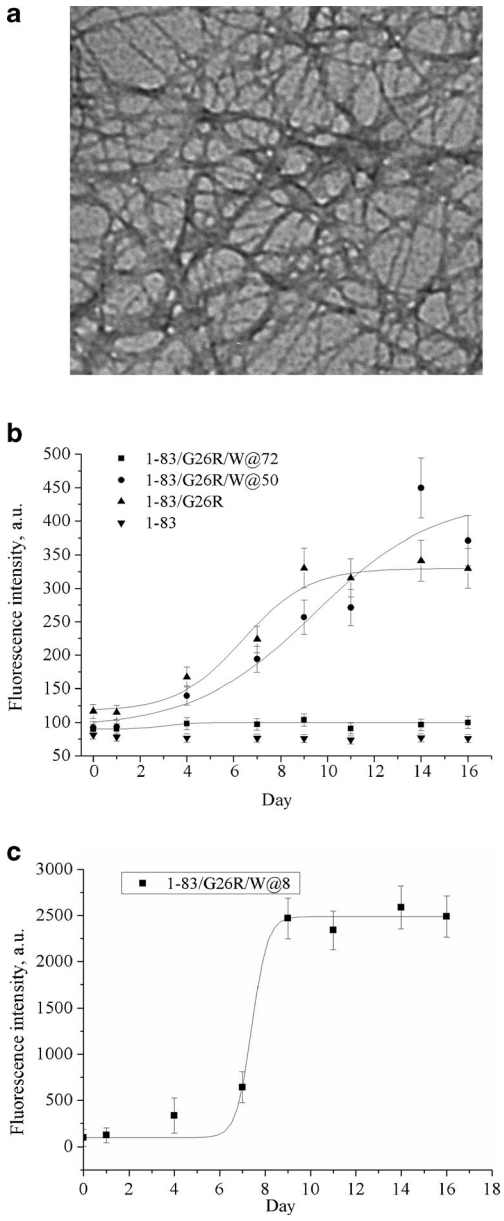

Fig. 1 TEM images of apoA-I 83 fibrils (**a**) and fibrillization kinetics of apoA-I variants monitored by measuring ThT fluorescence intensity at 484 nm (**b**, **c**). Protein concentration was 0.9 μM, ThT concentration was 6.9 μM

Influence of apoA-I Variants on the Membrane Polar Region

At the next step of the study, we employed the well-known fluorescent probe Laurdan to trace the impact of apoA-I variants on the polar region of the lipid bilayer. Within the membrane this probe protrudes its lauric acid tail in the acyl chain region of the lipid bilayer, while its fluorescing moiety locates at the glycerol level of the phospholipid headgroups [31]. The most remarkable spectral properties of Laurdan are high sensitivity to microenvironmental polarity and dependence of emission maximum on the extent of reorientation of the solvent dipoles around the excited state dipole of the probe [33,

34]. This feature of Laurdan manifests itself in the appearance of two clearly distinct components in the emission spectrum, which are attributed to solvent-unrelaxed (shorter wavelength band) and solvent-relaxed (longer wavelength band) states [34].

Figure 2 represents typical emission spectra of Laurdan in the lipid and lipid-protein systems. The first noticeable effect is that incorporation of sterol into PC bilayer modifies the shape of Laurdan spectra, producing blue shift of emission maximum and half-width reduction. Such cholesterol effect is generally explained by the lowered polarity and decreased relaxation rate of water molecules at hydrophobic/hydrophilic interface [35]. While examining Laurdan fluorescence in two lipid phases (gel and liquid-crystalline), Parasassi et al. assumed that restricted water mobility reflects decreased dynamics of phospholipids [34, 35]. A lot of mechanisms have been proposed to explain condensing effect of cholesterol on the lipid bilayer structure. Among them are the model of condensed complexes [36], super-lattice model [37], umbrella model [38] and template model [39]. Condensed complex model assumes that formation of Chol-lipid complexes results in membrane condensation because lipid acyl chains become more ordered. Super-lattice model suggests that inclusion of cholesterol induces the long-range order. Umbrella mechanism implies that small hydrophilic part of Chol molecule causes lipids to screen sterol from unfavorable contacts with water. This screening is possible only if lipid molecules straighten to create the space for cholesterol. Finally, according to the template model the flexible acyl chains of phospholipids ideally complement the planar nucleus of Chol to produce a high number of close hydrophobic contacts and tight packing.

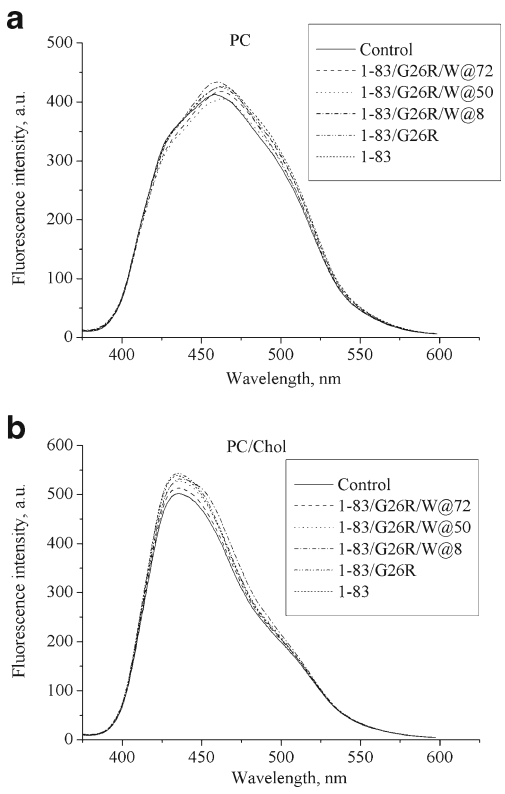

Fig. 2 Laurdan emission spectra in PC (**a**) and PC/Chol (**b**) liposomes in the absence and presence of aggregated apoA-I variants. Lipid concentration was 16 μM, protein concentration was 1 μM, Laurdan concentration was 0.6 μM

The environment-dependent spectral changes of Laurdan are generally described by a steady-state parameter termed generalized polarization (GP), calculated according to Eq. (1) [31]. GP value is related to the interaction between the interfacial water molecules and the probe moiety, and thus allows quantitative analysis of membrane polarity changes. As seen in Fig. 3a, in PC bilayer monomeric proteins produced GP increase by 13-16 %, with no clear differences between various mutants, while aggregated proteins provoked GP decrease, with the magnitude of this effect varying from ~25 to ~70 % (Fig. 3b). Moreover, GP decrease was found to be inversely correlated with the extent of fibril formation, i.e., with the maximum increase of ThT fluorescence. Accordingly, the least GP changes were revealed for 1-83/G26R/W@8, the protein displaying the highest fibrillization degree. Taken together, all the above tendencies led us to suppose that oligomeric forms of apoA-I mutants possess much more pronounced ability to cause GP decrease compared to fibrillar species. The decreased values of Laurdan generalized polarization is generally attributed to the increased water penetration in the lipid bilayer. One of the most probable reasons for the observed bilayer dehydration is decrease in lipid packing density due to surface defects in the membrane, induced by the sorption of apoA-I fibrils. These structural defects may represent the lipid uptake from the parent bilayer by the fiber, and formation of lipid-containing amyloid aggregates. Similar effects were observed for islet amyloid polypeptide [40, 41], oligomeric Aβ peptide [42], as well as for a variety of water-soluble proteins [43]. In contrast to PC bilayer, in PC/Chol model membranes relative GP changes were very small, no more than 6 % for all protein variants, thus being within the experimental error (Fig. 3c, d). These data imply that sterol hampers the ability of both monomeric and fibrillar peptides to alter the physicochemical properties of lipid-water interface. The rigidifying effect of the sterol on lipid bilayer structure, described above, underlies apparently the hindrance of the apoA-I penetration in Chol-containing membranes.

Effect of apoA-I Mutants on Lipid Bilayer Structure Probed by Pyrene

To trace the modifications in nonpolar membrane region induced by apoA-I variants, we employed classical membrane probe pyrene, widely used to characterize the dynamical properties of lipid bilayer. The fluorescence spectrum of this probe is featured by five vibronic bands whose relative intensities exhibit clear dependence on the polarity of fluorophore

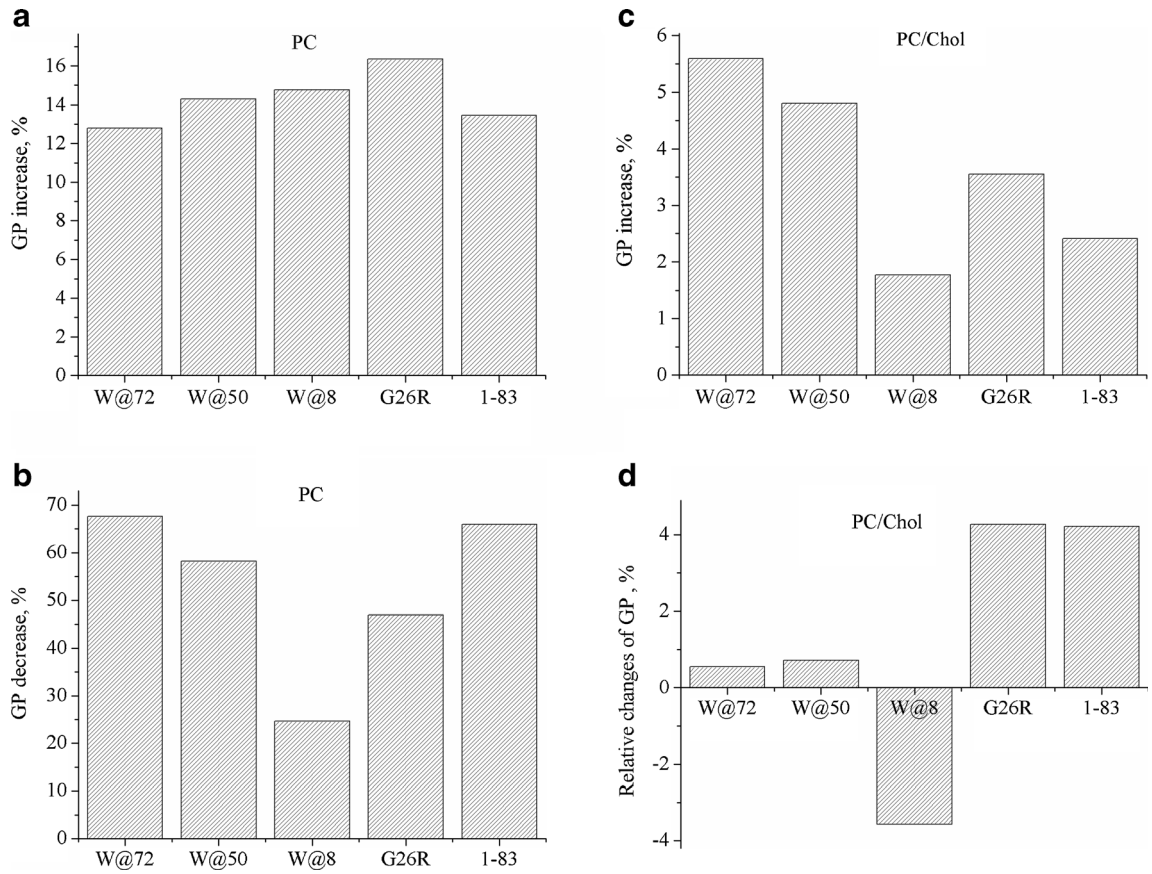

Fig. 3 Effect monomeric (**a**, **c**) and aggregated (**b**, **d**) apoA-I variants on generalized polarization of Laurdan in PC (**a**, **b**) and PC/Chol (**c**, **d**) liposomes

microenvironment (so-called "Ham effect", or *Py* scale) [44]. Specifically, the intensity of third vibronic peak (0–2 transition) is significantly enhanced in hydrophobic environment, while the intensity of first vibronic peak (0–0 transition) is markedly increased in polar media [45]. This pyrene characteristics allows employing the intensity ratio of the first-to-third vibronic band I_I/I_{III} as robust descriptor of polarity in the vicinity of the probe molecules. Accordingly, in water I_I/I_{III} was found to be 1.96, while in the solvents of lower polarity this ratio decreases reaching the value 0.6 in *n*-hexane [46, 47]. Another important pyrene spectral parameter is excimer-to-monomer intensity ratio (*E*/*M*). This parameter reflects the extent of pyrene excimerization, the process which is commonly analyzed within the framework of lipid bilayer free volume [48]. Membrane free volume characterizes the difference between the effective and van-der-Waals volumes of lipid molecules, and arises from the lateral displacement of hydrocarbon chain following the kink formation [49].

Figure 4 shows the typical emission spectra of pyrene in neat lipid vesicles (control line in the figure) and in the presence of apoA-I variants. It appeared that relative intensity of the first-to-third vibronic bands does not undergo any significant changes upon protein addition in all systems studied here. This implies that formation of protein-lipid contacts does not affect membrane polarity at the level of initial acyl chain carbons where pyrene monomers tend to reside. As for the *E*/*M* ratio, this parameter underwent slight changes in PC model membranes only upon addition of aggregated 1-83/G26R/W@50 and 1-83/G26R/W@72 (decrease by ~6 %) and monomeric 1–83 (increase by ~6 %) (Fig. 5). Obviously, the proteins do not exert any significant effect on the membrane free volume, and the observed *E*/*M* changes may reflect transversal redistribution of the probe molecules in the lipid bilayer upon protein-lipid interactions. Specifically, if oligomer or fibril binding results in the lipid uptake followed by the formation of membrane defects with increased hydration, nonpolar pyrene molecules might be expected to move in more hydrophobic regions to avoid the contacts with water. Contrary to PC vesicles, pyrene fluorescence spectra in PC/Chol membranes showed no clearly defined excimer peak (Fig. 4b). This implies that condensing effect of cholesterol hinders the probe lateral diffusion, thereby reducing the probability of collisions between pyrene monomer and decreasing the rate of excimer formation.

Discussion

Though the idea that apoA-I fibrillization is a key event in protein-related amyloidosis is generally accepted, the exact

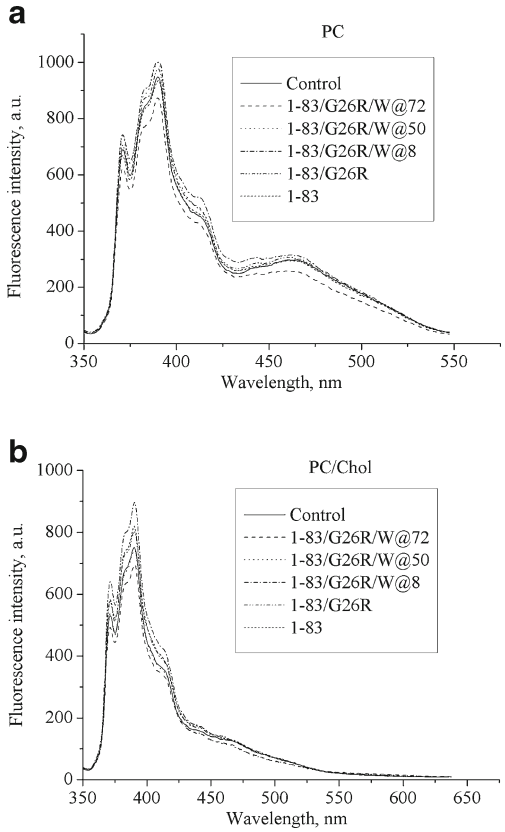

Fig. 4 Pyrene emission spectra in PC (**a**) and PC/Chol (**b**) liposomes in the absence (control) and presence of aggregated apoA-I variants. Lipid concentration was 16 μM, protein concentration was 1 μM, pyrene concentration was 0.1 μM

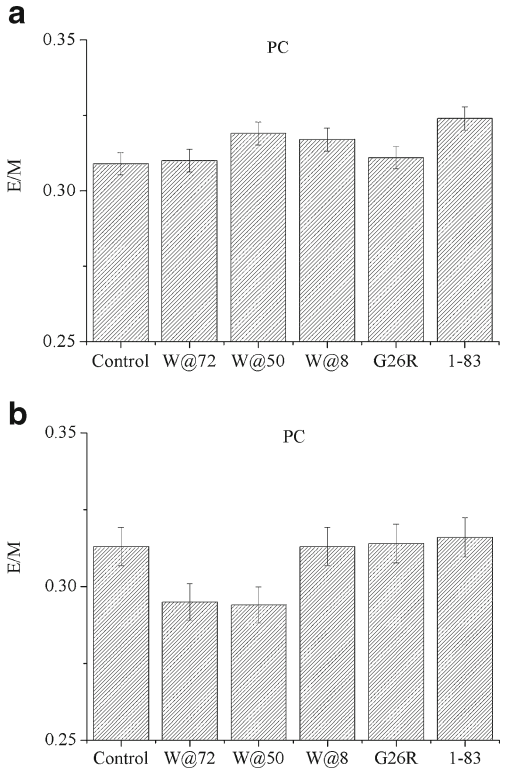

Fig. 5 Effect of monomeric (**a**) and aggregated (**b**) apoA-I variants on pyrene E/M ratio in PC liposomes

molecular mechanisms by which amyloid fibrils induce cell death still remain lacking. In the present work we explored membrane-modifying properties of amyloid fibrils from the mutated N-terminal apoA-I fragment. The analysis of pyrene excimerization process did not reveal noticeable alterations in the structural and dynamic properties of nonpolar bilayer region, suggesting that apoA-I mutants do not penetrate into the membrane hydrocarbon core. However, comparison of Laurdan GP values in different peptide-lipid systems showed that the examined apoA-I variants are capable of modifying the polar region of lipid bilayer. The GP changes observed for PC liposomes are indicative of the principal difference between monomeric and aggregated apo A-I variants in the pattern of membrane modification: oligomers and fibrils cause the rise in lipid bilayer hydration and reduction of the lipid packing density, while monomers evoke membrane dehydration and tighter packing of lipid headgroups. In contrast, PC/Chol vesicles were much less vulnerable to the action of both monomeric and aggregated apoA-I mutants. These finding are in concert with previously reported data highlighting the key role of cholesterol in preventing the lipid bilayer from disrupting influence of aggregated species [50–52]. The origin of such sterol effect was assumed to lie in its bilayer-rigidifying ability that hinders protein penetration into membrane interior, prevents ion channel formation and membrane disruption.

The extent of fibrillization degree and the impact of the apoA-I amyloid-like fibers on the stability of the lipid bilayer were found to depend on peptide variant type. Based on the results outlined here, it is difficult to say definitely whether the differences in fibrillization extent between apoA-I variants are associated with the nature of mutation or they result from the uncontrolled subtle variations in the experimental conditions. In this context it is sensible to refer to the work of Cecchini et al. where the role of Trp residues in myoglobin amyloidogenesis has been evaluated [53]. Accordingly, analysis of different protein variants, in which one or several Trp were substituted with Phe showed that position of Trp along the sequence affects the extent of aggregation. This may originate from the fact that Phe is unable to maintain the same long-range interactions as Trp does. When such substitution occurs in the regions of peptide sequence critical for amyloid formation, the overall aggregation potential of the protein reduces. Notably, the effect of mutation on the fibril-forming propensity of apoA-I fragment was recently analyzed by Adachi et al. [29]. Specifically, using the fluorescent probes ANS and ThT, the authors demonstrated that substitution of Gly by Lys residue in the position 26 slows down the kinetics of fibrillization. It was suggested that this mutation affects the intermolecular contacts between apoA-I monomers due to the different hydrogen-bonding capacity and relative hydrophobicity of Gly and Lys amino acids.

Table 2 Lipid binding regions of G26R apoA 83 peptide identified with HeliQuest

G26R (1–83) fragment	$<\mu H>$	z	D^*
$_{10}$RVKDLATVYVDVLKDSRR$_{27}$	0.457	1	0.76
$_{23}$KDSRRDYVSQFEGSALGK$_{40}$	0.114	0	0.43
$_{44}$LKLLDNWDSVTSTFSKLR$_{61}$	0.466	2	1.1
$_{52}$SVTSTFSKLREQLGPVTQ$_{69}$	0.422	0	0.73

* Lipid discrimination factor was calculated as $D=0.944(<\mu H>)+0.33z$ [*]

In the following, it was tempting to analyze what region of apoA-I N-terminal fragment may account for its membrane binding. Our previous studies of FRET between AV-PC and amyloid-specific dye Thioflavin T provided the arguments in favor of the existence of discrete lipid-binding sites within the structure of 1-83/G26R/W@8 fibrils [54]. It was supposed that fibril-membrane contact region contains the sequence Q41–S58. To verify this assumption, we employed HeliQuest online server yielding the mean hydrophobicity ($<H>$), hydrophobic moment (μH), net charge (z) and eventually lipid discrimination factor D, characterizing lipid binding affinity of a certain polypeptide fragment [55, 56]. Analysis of 1–83 apoA-I sequence showed that this peptide possesses four most probable membrane-binding regions, viz. R10–R27, K23–K40, L44–R61, S52–Q69, with the highest lipid-associating potential corresponding to L44–R61 (Table 2), consistent with the previous study of synthetic peptides corresponding to the apo A-I sequence [57]. Thus, it can be assumed that this region is responsible for fibril attachment to the surface of lipid vesicles.

To get more detailed information, liposome complexes with 1-83/G26R/W@8 fibrils were analyzed using transmission electron microscopy. Intact lipid vesicles showed smoothly rounded shapes in TEM images with the diameter *ca.* 50±2 nm (data not shown). Incubation of liposomes with G26R amyloid variants results in densely clustered lipid vesicles entangled with the fibrils. In most cases the surfaces of the fibers are colocalized with the lipid bilayer surface,

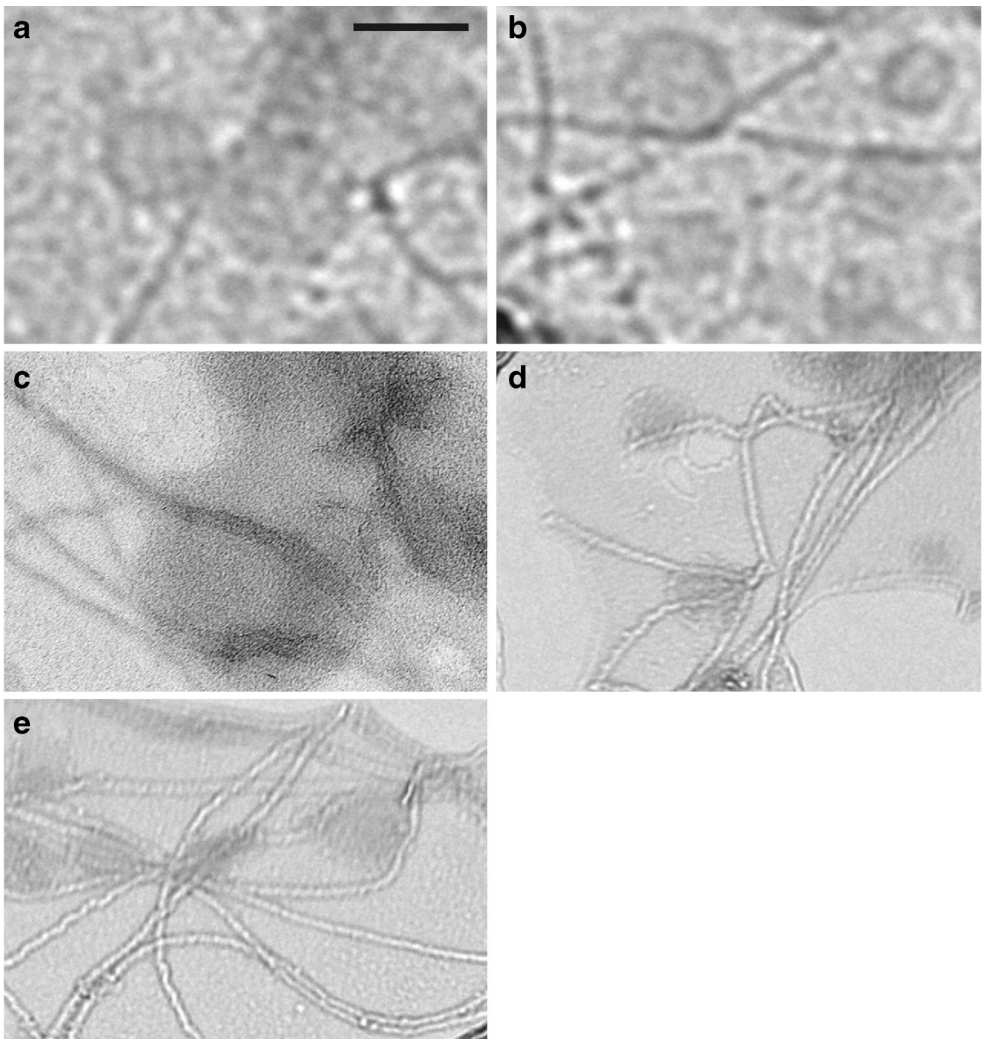

Fig. 6 Transmission electron micrographs of negatively stained 1-83/G26R/W@8 fibrils in the presence of PC liposomes. Scale bar is 50 nm

lending support to the idea of amyloid adsorption onto vesicles (Fig. 6a–c). Upon fibril association, the lipid vesicles conserve mainly the round shape, however, invaginations were also observed (Fig. 6e). In some cases amyloid fibers were gathered into the bundles around the liposomes (Fig. 6d, e). In addition, tiny vesicles were observed in contact with the fibrils or adherent to the native 50 nm liposomes (Fig. 6b, d, e). These small vesicles are evidently formed from the lipids, extracted by apoA 83 fibrillar aggregates from the parent bilayer. The sequence of events underlying the loss of membrane integrity is assumed to involve amyloid adsorption onto bilayer surface → membrane invagination and thinning → bilayer defragmentation and loss of structural stability. Specific fibril-lipid interactions, involving intercalation of protein wedge-shaped domains, were assumed to result in lipid bilayer destabilization and eventual extraction of the membranous material [58]. Milanesi et al. identified such mode of fibril-liposome interactions as a specific membrane distortion by a peptide/protein self-assembly different from previously observed mechanisms of lipid bilayer disruption [59].

Conclusions

To summarize, fluorescent probes Laurdan and pyrene proved to be suitable for monitoring the perturbations in membrane structure provoked by apoA-I mutants. The present study provides evidence for modifying effect of monomeric and aggregated (oligomeric and fibrillar) variants of apoA-I N-terminal fragment on the molecular organization of the polar part of lipid bilayer, with acyl chain region remaining virtually unaffected. Cholesterol proved to be capable of preventing the lipid bilayer from destabilizing action of apoA-I mutants. The observed increase in bilayer hydration and lipid disordering produced by aggregated species may represent one of the pathways of apoA-I amyloid cytotoxicity.

Acknowledgments This work was supported by the grant from Fundamental Research State Fund of Ukraine (project number F54.4/015) and Grant-in-Aid for Scientific Research 25293006 (to H.S.) from the Japan Society for the Promotion of Science.

References

1. Fink AL (1998) Protein aggregation: folding aggregates, inclusion bodies and amyloid. Fold Des 3:R9–R23
2. Serpell LC (2000) Alzheimer's amyloid fibrils: structure and assembly. Biochim Biophys Acta 1502:16–30
3. Gorbenko GP, Kinnunen PKJ (2006) The role of lipid–protein interactions in amyloid-type protein fibril formation. Chem Phys Lipids 141:72–82
4. Zerovnik E (2002) Amyloid-fibril formation. Proposed mechanisms and relevance to conformational disease. Eur J Biochem 269:3362–3371
5. Dobson CM (2003) Protein folding and misfolding. Nature 426:884–890
6. Lu JX, Qiang W, Yau WM, Schwieters CD, Meredith SC, Tycko R (2000) Molecular structure of β-amyloid fibril in Alzheimer's disease brain issue. Cell 154:1257–1268
7. Aisenbrey C, Borowik T, Byström R, Bokvist M, Lindström F, Misiak H, Sani M, Gröbner G (2008) How is protein aggregation in amyloidogenic diseases modulated by biological membranes? Eur Biophys J 37:247–255
8. Arispe N, Rojas E, Pollard H (2003) Alzheimer's disease amyloid beta protein forms calcium channels in bilayer membranes: blockade by tromethamine and aluminium. Pro Natl Acad Sci 89:10940–10944
9. Gorbenko GP, Trusova VM (2011) Protein aggregation in a membrane environment. Adv Protein Chem Struct Biol 84:114–142
10. Bucciantini M, Cecchi C (2010) Biological membranes as protein aggregation matrices and targets of amyloid toxicity. Methods Mol Biol 648:231–243
11. Bucciantini M, Rigacci S, Stefani M (2014) Amyloid aggregation: role of biological membranes and the aggregate-membrane system. J Phys Chem Lett 5:517–527
12. Demuro A, Mina E, Kayed R, Milton SC, Parker I, Glabe CG (2005) Calcium dysregulation and membrane disruption as a ubiquitous neurotoxic mechanism of soluble amyloid oligomers. J Biol Chem 280:17294–17300
13. Lashuel HA, Lansbury PT (2006) Are amyloid diseases caused by protein aggregates that mimic bacterial pore-forming toxins? Q Rev Biophys 39:167–201
14. Smith P, Brender J, Ramamoorthy A (2009) The induction of negative curvature as a mechanism of cell toxicity by amyloidogenic peptides. The case of islet amyloid polypeptide. J Am Chem Soc 131:4470–4478
15. de Planque RR, Raussen V, Contera SA, Rijkers DTS, Liskamp RMJ, Ruysschaert JM, Ryan JF, Separovic F, Watts A (2007) β-sheet structured β-amyloid (1–40) perturbs phosphatidylcholine model membranes. J Mol Biol 368:982–987
16. Lee CC, Sun Y, Huang H (2012) How type II diabetes-related islet amyloid polypeptide damages lipid bilayers. Biophys J 102:1059–1068
17. Verdier Y, Zarandi M, Penke B (2004) Amyloid beta-peptide interactions with neuronal and glial cell plasma membrane: binding sites and implications for Alzheimer's disease. J Pept Sci 10:229–248
18. Sciacca MF, Brender JR, Lee DK, Ramamoorthy A (2012) Phosphatidylethanolamine enhances amyloid-fiber dependent membrane fragmentation. Biochemistry 51:7676–7684
19. Butterfield DA, Castegna A, Lauderback CM, Drake J (2002) Evidence that amyloid beta-peptide-induced lipid peroxidation and its sequelae in Alzheimer's disease brain contribute to neuronal death. Neurobiol Aging 23:655–664
20. Obici L, Franceschini G, Calabresi L, Giorgetti S, Stoppini M, Merlini G, Bellotti V (2006) Structure, function and amyloidogenic propensity of apolipoprotein A-I. Amyloid 13:191–205
21. Rosenson RS, Brewer HB Jr, Davidson WB, Fayad ZA, Fuster V, Goldstein J, Hellerstein M, Jiang XC, Phillips MC, Rader DJ, Remaley AT, Rothblat GH, Tall AR, Yvan-Charvet L (2012) Cholesterol efflux and atheroprotection: advancing the concept of reverse cholesterol transport. Circulation 125:1905–1919
22. Phillips MC (2013) New insights into the determination of HDL structure by apolipoproteins: thematic review series: high density lipoprotein structure, function, and metabolism. J Lipid Res 54:2034–2048
23. Genschel J, Haas R, Propsting MJ, Schmidt H (1998) Apolipoprotein A-I induced amyloidosis. FEBS Lett 430:145–149

24. Monti DM, Guglielmi F, Monti M, Cozzlino F, Torrassa S, Relini A, Pucci P, Arciello A, Piccoli R (2010) Effects of a lipid environment on the fibrillogenic pathway of the N-terminal polypeptide of human apolipoprotein a-I, responsible for in vivo amyloid fibril formation. Eur Biophys J 39:1289–1299
25. Adachi E, Kosaka A, Tsuji K, Mizuguchi C, Kawashima H, Shigenaga A, Nagao K, Akaji K, Otaka A, Saito H (2014) The extreme N-terminal region of human apolipoprotein A-I has a strong propensity to form amyloid fibrils. FEBS Lett 588:389–394
26. Lagerstedt JO, Cavigiolio G, Roberts LM, Hong HS, Jin LW, Fitzgerald PG, Oda MN, Voss JC (2007) Mapping the structural transition in an amyloidogenic apolipoprotein A-I. Biochemistry 46:9693–9699
27. Chetty PS, Ohshiro M, Saito H, Dhanasekaran P, Lund-Katz S, Mayne L, Englander W, Phillips MC (2012) Effect of the Iowa and Milano mutations on the apolipoprotein A-I structure and dynamics determined by hydrogen exchange and mass spectrometry. Biochemistry 51:8993–9001
28. Das M, Mei X, Jayaraman S, Atkinson D, Gursky O (2014) Amyloidogenic mutations in human apolipoprotein A-I are not necessarily destabilizing—a common mechanism of apolipoprotein A-I misfolding in familial amyloidosis and atherosclerosis. FEBS J 281: 2525–2542
29. Adachi E, Nakajima H, Mizuguchi C, Dhanasekaran P, Kawashima H, Nagao K, Akaji K, Lund-Katz S, Phillips MC, Saito H (2013) Dual role of an N-terminal amyloidogenic mutation in apolipoprotein A-I: destabilization of helix bundle and enhancement of fibril formation. J Biol Chem 288:2848–2856
30. Groenning M (2010) Binding mode of Thioflavin T and other molecular probes in the context of amyloid fibrils—current status. J Chem Biol 3:1–18
31. Parasassi T, Krasnowska EK, Bagatolli L, Gratton E (1998) Laurdan and Prodan as polarity-sensitive fluorescent membrane probes. J Fluoresc 8:365–373
32. Girych M, Gorbenko G, Trusova V, Adachi E, Mizuguchi C, Nagao K, Kawashima H, Akaji K, Phillips M, Saito H (2014) Interaction of thioflavin T with amyloid fibrils of apolipoprotein A-I N-terminal fragment: resonance energy transfer study. J Struct Biol 185:116–124
33. Sanchez SA, Tricerri MA, Gratton E (2012) Laurdan generalized polarization fluctuations measures membrane packing micro-heterogeneity in vivo. Proc Natl Acad USA 109:7314–7319
34. Parasassi T, Stasio GD, Ravagnan G, Rusch RM, Gratton E (1991) Quantification of lipid phases in phospholipid vesicles by the generalized polarization of Laurdan fluorescecne. Biophys J 60:179–189
35. Parasassi T, Stefano M, Loiero M, Ravagnan G, Gratton E (1994) Influence of cholesterol on phospholipid bilayer phase domains as detected by Laurdan fluorescence. Biophys J 66:120–132
36. McConnell HM, Radhakrishnan A (2003) Condensed complexes of cholesterol and phospholipids. Biochim Biophys Acta 1610:159–173
37. Huang J (2002) Exploration of molecular interactions in cholesterol superlattices: effect of multibody interactions. Biophys J 83:1014–1025
38. Dai J, Alwarawrah M, Huang J (2010) Instability of cholesterol clusters in lipid bilayers and the cholesterol's umbrella effect. J Phys Chem B 114:840–859
39. Daly T, Wang M, Regen SL (2011) The origin of cholesterol's condensing effect. Langmuir 27:2159–2161
40. Domanov Y, Kinnunen PKJ (2008) Islet amyloid polypeptide forms rigid lipid-protein amyloid fibrils on supported phospholipid bilayers. J Mol Biol 376:42–54
41. Sparr E, Engel M, Sakharov D, Sprong M, Jacobs J, de Kruijff B, Höppener J, Killian JA (2004) Islet amyloid polypeptide-induced membrane leakage involves uptake of lipids by forming amyloid fibers. FEBS Lett 577:117–120
42. Michikawa M, Gong JS, Fan QW, Sawamura N, Yanagisawa K (2001) A novel action of Alzheimer's amyloid β-protein (Aβ): oligomeric Aβ promoted lipid release. J Neurosci 21:7226–7235
43. Zhao H, Tuominen EKJ, Kinnunen PKJ (2004) Formation of amyloid fibers triggered by phosphatidylserine-containing membranes. Biochemistry 43:10302–10307
44. Loura LM, do Canto AM, Martins J (2013) Sensing hydration and behavior of pyrene in POPC and POPC/cholesterol bilayers: a molecular dynamics study. Biochim Biophys Acta 1828:1094–1101
45. Kalyanasundaram K, Thomas JK (1977) Environmental effects on vibronic band intensities in pyrene monomer fluorescence and their application in studies of micellar systems. J Am Chem Soc 99:2039–2044
46. Karpovich DS, Blanchard GJ (1995) Relating the polarity-dependent fluorescence response to vibronic coupling. Achieving a fundamental understanding of the py polarity scale. J Phys Chem 99:3951–3958
47. Tedeshi C, Mohwald H, Kirstein S (2001) Polarity of layer-by-layer deposited polyelectrolyte films as determined by pyrene fluorescence. J Am Chem Soc 123:954–960
48. Ioffe VM, Gorbenko GP (2005) Lysozyme effect on structural state of model membranes as revealed by pyrene excimerization studies. Biophys Chem 114:199–204
49. Kinnunen PKJ, Koiv A, Lehtonen JYA, Mustonen P (1994) Lipid dynamics and peripheral interactions of proteins with membrane surfaces. Chem Phys Lett 73:181–207
50. Cecchi C, Baglioni S, Fiorillo C, Pensalfini A, Liguri G, Nosi D, Rigacci S, Bucciantini M, Stefani M (2005) Insights into the molecular basis of the differing susceptibility of varying cell types to the toxicity of amyloid aggregates. J Cell Sci 118:3459–3470
51. Muller WE, Kirsch C, Eckert G (2001) Membrane-disordering effects of β-amyloid peptides. Biochem Soc Trans 29:617–624
52. Kastorna A, Trusova V, Gorbenko G, Kinnunen P (2012) Membrane effects of lysozyme amyloid fibrils. Chem Phys Lipids 165:331–337
53. Cecchini P, Franceschi G, Frare E, Fontana A, de Laureto P (2012) The role of tryptophan in protein fibrillogenesis: relevance of Trp7 and Trp14 to the amyloidogenic properties of myoglobin. Protien Eng Des Sel 25:199–203
54. Girych M, Maliyov I, Romanova M, Gorbenko G, Adachi E, Mizuguchi C, Molotkovsky J, Saito H (2013) Fluorescence energy transfer study of the lipid bilayer interactions with truncated apolipoprotein A-I mutants. Biophys Bull 29:39–50
55. Gautier R, Douguet D, Antonny B, Drin G (2008) HeliQuest: a web server to screen sequences with specific alpha-helical properties. Bioinformatics 24:2101–2102
56. Keller R (2011) New user-friendly approach to obtain an Eisenberg plot and its use as a practical tool in protein sequence analysis. Int J Mol Sci 21:5577–5591
57. Palgunachari MN, Mishra VK, Lund-Katz S, Phillips MC, Adeyeye SO, Alluri S, Anantharamaiah GM, Segrest JP (1996) Only the two end helixes of eight tandem amphipathic helical domains of human apo A-I have significant lipid affinity. Implications for HDL assembly. Arterioscler Thromb Vasc Biol 16:328–338
58. Boucrot E, Pick A, Camdere G, Liska N, Evergren E, McMahon HT, Kozlov M (2012) Membrane fission is promoted by insertion of amphipathic helices and is restricted by crescent BAR domains. Cell 149:124–136
59. Milanesi L, Sheynis T, Xue WF, Orlova EV, Hellewell AL, Jelinek R, Hewitt EW, Radford S, Saibil HR (2012) Direct three-dimensional visualization of membrane disruption by amyloid fibrils. Proc Natl Acad Sci 109:20455–20460